Theor Chem Acc (2003) 110: 345–351
DOI 10.1007/s00214-003-0476-9

Theoretical
Chemistry Accounts

Regular article

A theoretical study of radical-only and combined radical/carbocationic mechanisms of arachidonic acid cyclooxygenation by prostaglandin H synthase

Pedro J. Silva[1], **Pedro A. Fernandes**[2], **Maria João Ramos**[2]

[1] Fac. de Ciências da Saúde, Univ. Fernando Pessoa, Rua Carlos da Maia 296, 4200-150, Porto, Portugal
[2] REQUIMTE, Faculdade de Ciências do Porto, Rua do Campo Alegre 687, 4169-007, Porto, Portugal

Received: 28 May 2003 / Accepted: 11 June 2003 / Published online: 11 November 2003

Abstract Prostaglandin H synthase catalyzes the oxygenation of arachidonic acid into the cyclic endoperoxide, prostaglandin G_2 (PGG_2), and the subsequent reduction of PGG_2 to the corresponding alcohol, prostaglandin H_2 (PGH_2), the precursor of all prostaglandins and thromboxanes. Both radical abstraction by a neighboring tyrosyl radical and combined radical/carbocationic models have been proposed to explain the cyclooxygenase part of this reaction. We have used density functional theory calculations to study the mechanism of the formation of the cyclooxygenated product PGG_2. We found an activation free energy for the initial hydrogen abstraction by the tyrosine radical of 15.6 kcal/mol, and of 14.5 kcal/mol for peroxo bridge formation, in remarkable agreement with the experimental value of 15.0 kcal/mol. Subsequent steps of the radical-based mechanism were found to happen with smaller barriers. A combined radical/carbocation mechanism proceeding through a sigmatropic hydrogen shift was ruled out, owing to its much larger activation free energy of 36.5 kcal/mol. Supplementary material is available in the online version of this article at http://dx.doi.org/10.1007/s00214-003-0476-9.
Electronic Supplementary Material Supplementary material is available in the online version of this article at http://dx.doi.org/10.1007/s00214-003-0476-9

Keywords: Cyclooxygenase – Mechanism – Radical – Carbocation – Density functional theory

Correspondence to: M. João Ramos
e-mail: mjramos@fc.up.pt

Introduction

Prostaglandin H synthases (PGHS) catalyze the first two steps in the biosynthesis of all prostaglandins and thromboxanes. These steps occur at two distinct, yet interacting, active sites: in the cyclooxygenase site, arachidonic acid is converted into the hydroperoxy endoperoxide prostaglandin G_2 (PGG_2), which is subsequently reduced to the corresponding alcohol, PGH_2, in the heme-containing peroxidase site [1, 2]. Many lipid-signaling agents derived from PGH_2 are important modulators of cardiovascular, gastrointestinal, renal, and reproductive function, as well as crucial mediators of inflammation, fever, and allergy. COX-2 (one of the two PGHS isoenzymes present in human tissues) has been implicated in some forms of colon cancer, and a substantial amount of research is currently focused on the discovery of COX-2 specific inhibitors [3]. A solid understanding of the common features in both isoenzymes' mechanisms is therefore required.

The crystal structure of ovine PGHS-1 complexed to arachidonic acid shows that the cyclooxygenase active site is mostly a L-shaped hydrophobic channel, with 19 active-site residues contacting the fatty acid substrate [4] (Fig. 1). Thuresson et al. [5] have undertaken a thorough side-directed mutagenesis study of these active-site residues, and have shown that only Tyr385 seems to be directly involved in catalysis. The other residues are mainly involved in binding arachidonic acid and positioning it in the right conformation so that PGG_2 rather than hydroperoxide side products are formed.

The initial proposal of the mechanism for the cyclooxygenase reaction by Hamberg and Samuelsson [6] is

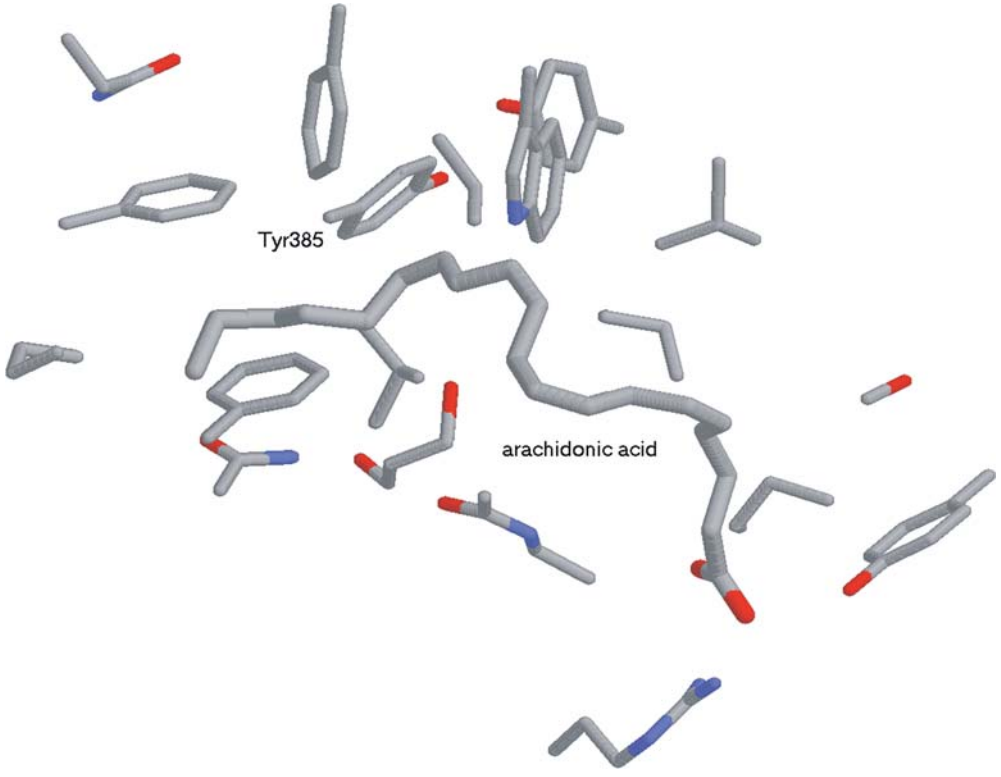

Fig. 1. X-ray structure of arachidonic acid bound to the cyclooxygenase active site [5]

shown in Fig. 2. In this mechanism, a protein-based radical abstracts the 13-pro-S hydrogen from bound arachidonic acid, yielding a C11–C15 delocalized pentadienyl radical. The radical sequentially reacts with two molecules of O_2, yielding the bicyclic hydroperoxide, PGG_2. A number of important findings support the basic tenets of the overall mechanism: the identification of a tyrosyl radical as the initiator of catalysis [7], the determination of X-ray structures of arachidonic acid bound at the active site of the protein [4], and the detection of a substrate-based pentadienyl radical by electron paramagnetic resonance spectroscopy [8].

Dean and Dean [9] suggested that the exquisite stereospecificity of the cyclooxygenase reaction, which introduces five chiral centers in an achiral molecule, could be explained by the formation of a carbocation center at C10. This would be produced after a sigmatropic hydrogen shift from C10 to the radical present in C13, which yields a C8–C12 delocalized pentadienyl radical (Fig. 2). Loss of an electron from this radical yields a carbocation that may cyclize under orbital symmetry control necessarily yielding a product with the required stereochemistry. After cyclization, the carbocation would again be reduced to the radical and the reaction would proceed as in the radical-only pathway.

The observed pentadienyl radical has been shown to encompass the C11–C15 carbons instead of the C8–C12 ones [10], which does not support the combined radical/carbocation mechanism. However, it is still possible that the observed radical is thermodynamically but not kinetically favored, and that cyclooxygenation proceeds more readily through the radical/carbocation mechanism. We have performed a theoretical study on both mechanisms, thus elucidating the correct one.

Methods

We modeled the C7–C16 atoms of arachidonic acid, where all relevant chemistry occurs, as (*Z*, *Z*, *Z*)-2,5,8-decatriene. Since mutagenesis studies [5] suggest that only Tyr385 is directly involved in the mechanism, we discarded all other active-site residues in order to lower the computational cost. In the reactions with the tyrosyl radical, the fatty acid model was further shortened in order to lower the computational cost. All the calculations were performed at the Becke3LYP level of theory [11, 12, 13]. In geometry optimizations a medium-sized basis set, 6-31G(d), was used, since it is well known that larger basis sets give very small additional corrections to the geometries, and their use for this end is hence considered unnecessary from a computational point of view [14, 15, 16, 17]. Accurate energies of the optimized geometries were calculated with a triple-ζ-quality basis set, 6-311 + G(3df,2p). Frequency analyses were performed at each stationary point on the potential-energy surface. All minima and transition states were identified by the number of imaginary frequencies. Thereafter the transition states were verified to connect the reactants and products of interest through internal reaction coordinate calculations. A scaling factor of 0.9804 was used for the frequencies. Zero-point and thermal effects (298.15 K, 1 bar) were added to the calculated energies, and also analyzed separately. The polarizable conductor model [18], as implemented in Gaussian98 [19], was used in order to account for the effects of the protein environment. The dielectric constant was chosen to be 4, as commonly used for the active site of proteins [20], although the results are quite insensitive to the exact value of this empirical parameter. Atomic charge and spin density distributions were calculated with a Mulliken population analysis [21], using the larger basis set. All calculations were performed with the Gaussian98 suite of programs [19].

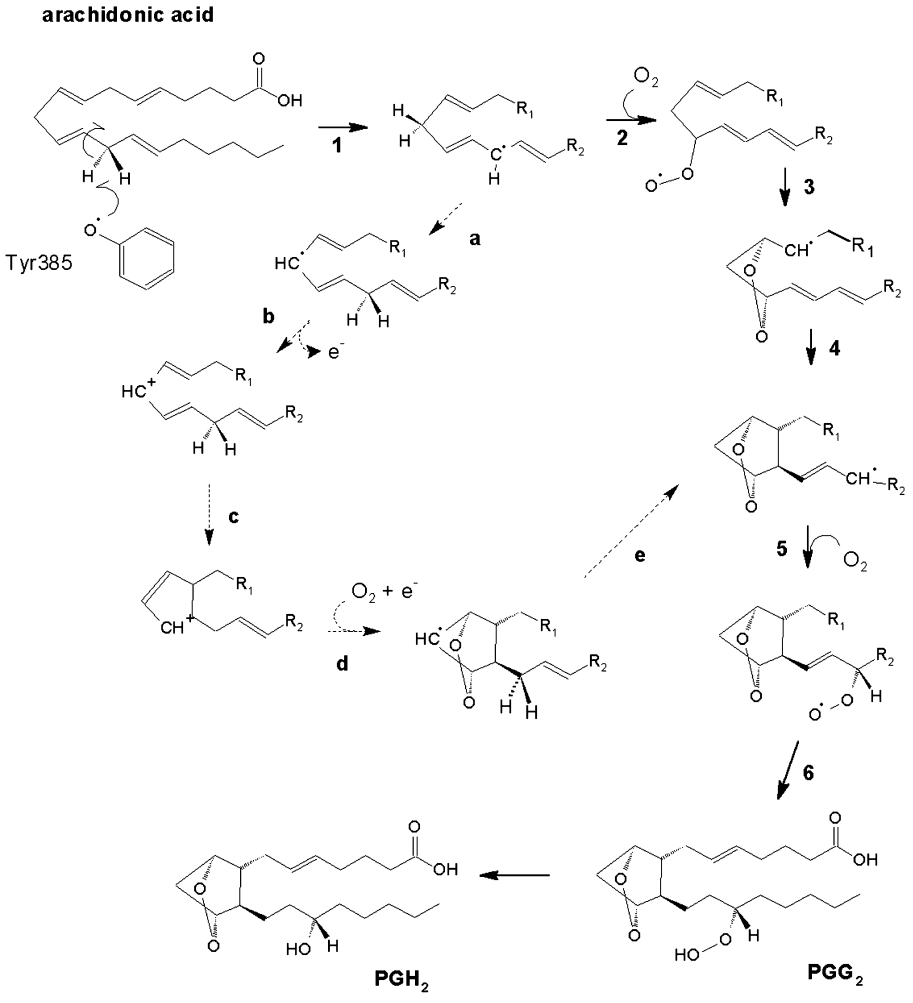

Fig. 2. Radical-only versus combined carbocation/radical mechanisms of arachidonic acid cyclooxygenation. Steps in the radical-only mechanism are *numbered* and shown with *solid arrows*. Steps characteristic of the combined carbocation/radical mechanism are *labeled alphabetically* and depicted with *dashed arrows*. $R_1 = –CH=CH–(CH_2)_3–COOH$; $R_2 = –(CH_2)_3–CH_3$

Results

Step 1. 13-pro-S hydrogen abstraction by Tyr385

According to both proposals, the first step in the cyclooxygenase mechanism should be the abstraction of the 13-pro-S hydrogen by Tyr385, as depicted in Fig. 3, where (*Z*, *Z*)-2,5-heptadiene models the C10–C16 moiety of the substrate and a phenoxy radical models the tyrosyl side chain. At the transition state, the abstracted hydrogen lies at almost equal distances from C13 and Tyr385 oxygen. The spin density, which in the reactants was fully localized in Tyr385, is now more evenly distributed between the fatty acid substrate (0.54) and the tyrosine residue (0.42). Almost no spin density is present in the transferred 13-pro-S hydrogen, showing that the process is a coupled proton–electron transfer (as seen in lipooxygenase [22]), rather than a pure hydrogen-atom transfer. In the products, the spin is fully delocalized across the substrate C11–C15 atoms. The activation Gibbs free energy of this reaction is 15.6 kcal/mol, in excellent agreement with the experimentally derived value of 15.0 kcal/mol (calculated from the data in Ref. [23]).

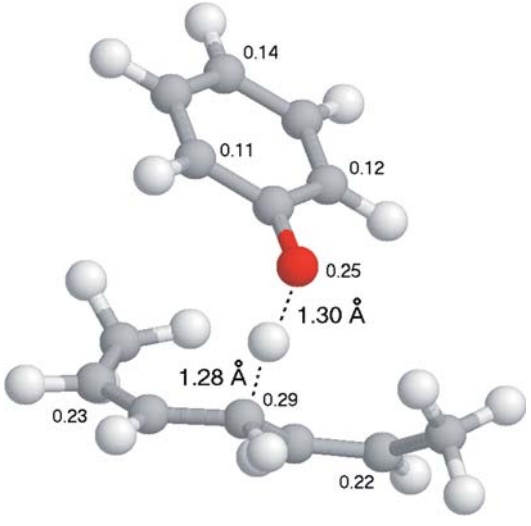

Fig. 3. Optimized transition state geometry for reaction 1. Relevant distances (angstroms) and spin densities larger than 0.10 in absolute value (atomic units) are depicted. The leftmost carbon atom corresponds to C16 in arachidonic acid

Step 2. Oxygen addition to C11

According to the radical-only mechanism, after the first step oxygen attack occurs at the C11 atom, yielding a peroxy radical. The reaction is depicted in Fig. 4. In the transition state (Fig. 4a), the O_2 molecule is located 2.11 Å from C11 and large spin densities are present both at the inner and at the outer oxygen atoms (0.69 and 0.72, respectively), with smaller spins at the C12–C15 carbon atoms. As the C–O distance finally reduces to 1.48 Å in the products, the spin becomes mostly localized on the outer oxygen atom (Fig. 4b). The activation Gibbs free energy of this step is 12.3 kcal/mol and the reaction is essentially reversible, with an overall decrease of free energy of −1.4 kcal/mol.

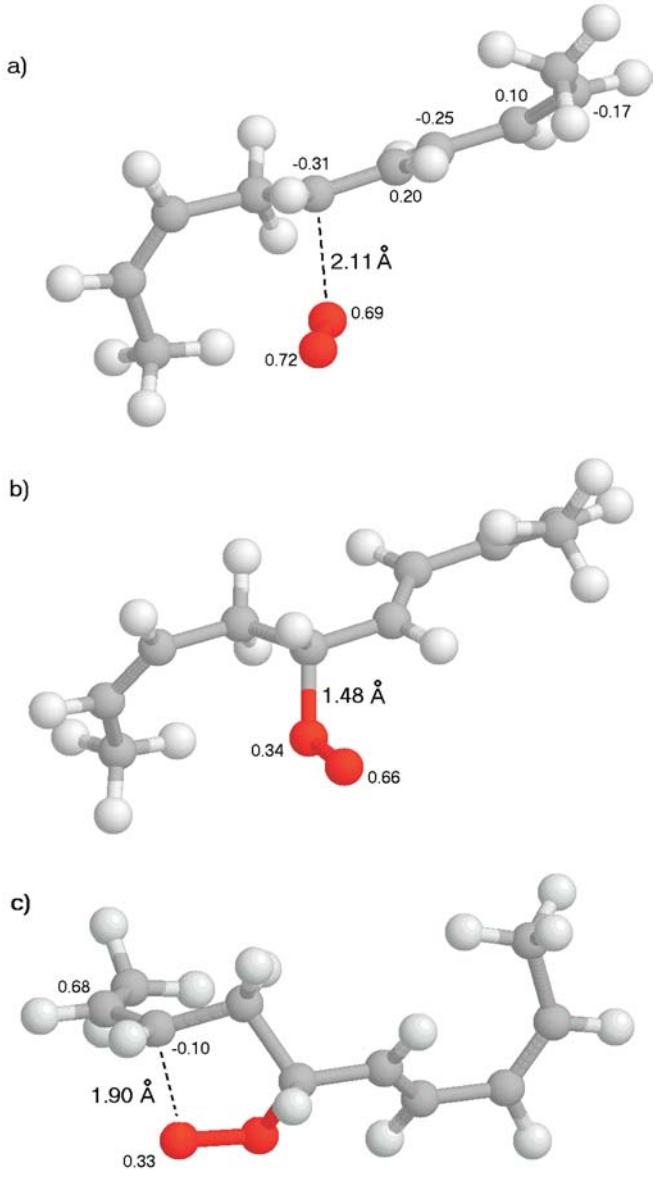

Fig. 4a–c. Reactions of the first oxygen molecule with arachidonic acid. **a** Optimized transition-state geometry for reaction 2. **b** Optimized product geometry for reaction 2. **c** Optimized product geometry for reaction 3. Relevant distances (angstroms) and spin densities larger than 0.10 in absolute value (atomic units) are depicted. In every structure, the left end of the molecule corresponds to the C7 atom

Step 3. Endoperoxide formation

A 69° clockwise rotation of the peroxy radical along the C–O bond axis brings the radical-containing outer oxygen atom into the correct position for the attack on C9. This rotation increases the free energies of the reagents by only 0.3 kcal/mol. In the transition state (Fig. 4c), the outer oxygen atom is located 1.90 Å from C9 and the electron spin is already quite delocalized back into the carbon chain (0.68 in C8). The activation Gibbs free energy of this step is 14.5 kcal/mol and the reaction is slightly unfavorable thermodynamically, with an increase of free energy of 4.2 kcal/mol.

Step 4. C–C bond formation

The local minimum we obtained by following the internal reaction coordinate in step 3 is not the most stable conformation: in order to yield PGG_2 with the right stereochemistry, a small rotation of this product to a lower minimum must occur. This new minimum lies 2.4 kcal/mol lower in the free-energy potential surface. As in the previous step, the energy barrier for this rotation is expected to be easily overcome by thermal effects. This species (Fig. 5a) is essentially a C8-based radical, which reacts with C12, thereby introducing a new C–C bond in the molecule. In the transition state (Fig. 5b) the C8–C12 distance has reduced from the initial value of 4.20 to 2.38 Å, still 50% longer than the final C–C bond distance. As the reaction moves to completion, electron spin eventually delocalizes to the C13–C15 portion of the substrate (0.70 in C13, −0.30 in C14, and 0.66 in C15). The activation free energy of this step is 12.2 kcal/mol and the reaction is quite favorable with $\Delta G = -10.1$ kcal/mol.

Step 5. Addition of the second oxygen molecule

Addition of an oxygen molecule to the si face of C15 yields the peroxy radical of PGG_2 (Fig. 5d). A stepwise increase of this C–O bond revealed a first-order saddle point when the O_2 molecule is 2.36 Å from C15 (Fig. 5c). The activation free energy of this step is very small, 1.6 kcal/mol, arising mostly from the loss of entropy due to the decrease of O_2 translational and rotational degrees of freedom. Indeed, the activation ΔH is actually negative (−8.3 kcal/mol), showing that the reaction is mostly diffusion-controled. The reaction is spontaneous with $\Delta G = -8.0$ kcal/mol. The large energy differences between the addition of the two O_2 molecules

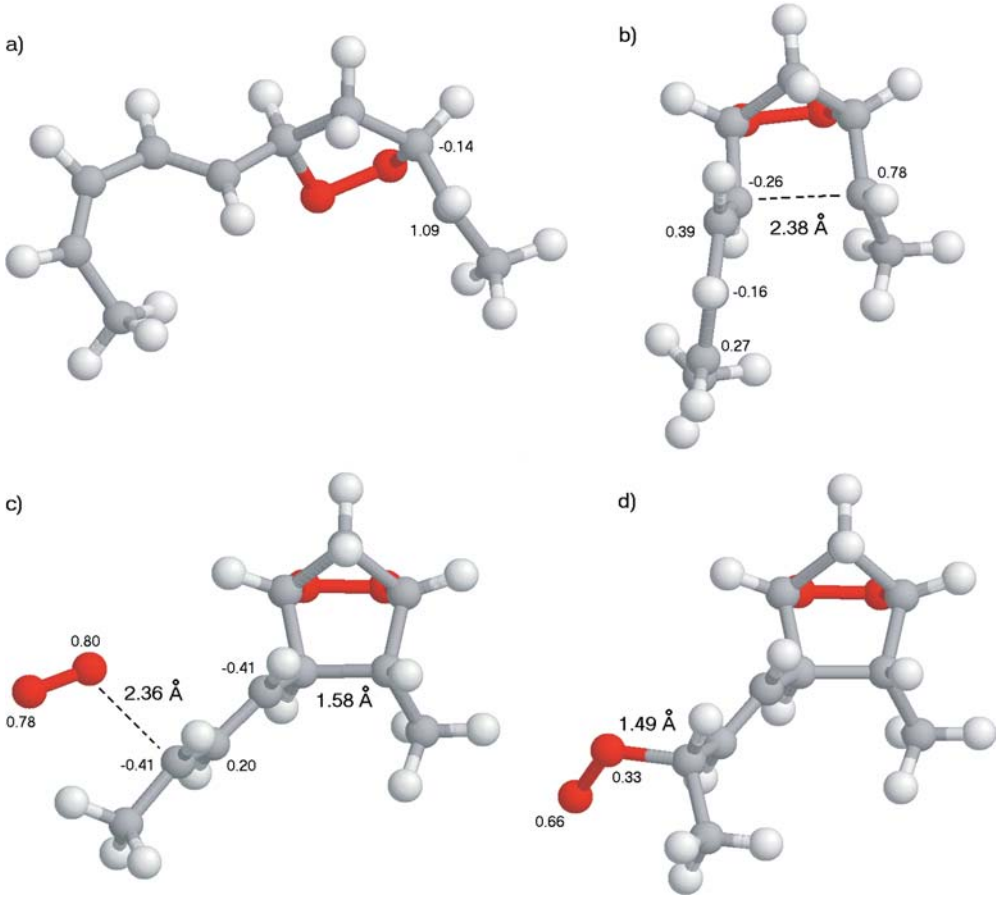

Fig. 5a–d. Closing of the cyclopentane ring and incorporation of the second oxygen atom. **a** Optimized reagent geometry for reaction 4. **b** Optimized transition-state geometry for reaction 4. **c** Optimized transition-state geometry for reaction 5. **d** Optimized product geometry for reaction 5. Relevant distances (angstroms) and spin densities larger than 0.10 in absolute value (atomic units) are depicted. In every structure, the leftmost carbon atom corresponds to C16 of the substrate

are not surprising, and are due to the smaller reactivity of the more delocalized radical present in step 2.

Step 6. Hydrogen abstraction from Tyr385 by the peroxy radical

The final step in the mechanism is hydrogen-atom abstraction from Tyr385 by the peroxy radical, which regenerates the tyrosyl radical for a new round of catalysis. We used a truncated model for the prostaglandin substrate, including only its C12–C16 moiety, since electronic effects from the cyclopentane ring should not affect the chemistry at the outer peroxydic oxygen in C15. As in step 1, a phenoxy radical models the tyrosyl side chain. At the transition state, the abstracted hydrogen lies at almost equal distances from Tyr385 oxygen and the outer peroxydic oxygen (Fig. 6). The electron spin, which in the reactants was largely located at this oxygen, has now migrated largely to the tyrosine residue. As in the first hydrogen transfer almost no spin is present in the transferred hydrogen, showing that this process is also a coupled proton–electron transfer, rather than a pure hydrogen-atom abstraction. In the products, the spin is fully delocalized in the tyrosine residue. The activation free energy is 12.8 kcal/mol and the reaction has $\Delta G = -0.2$ kcal/mol.

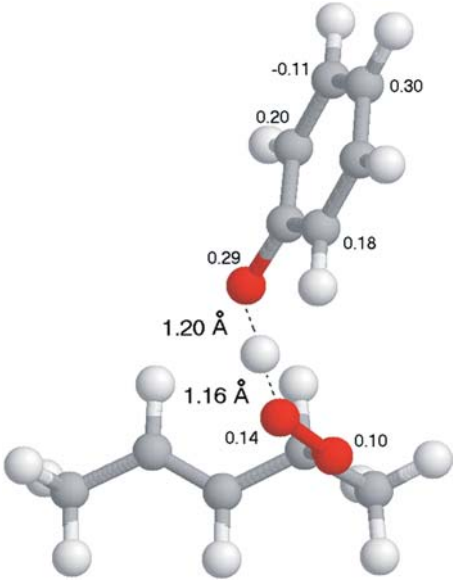

Fig. 6. Regeneration of the tyrosyl radical. Optimized transition-state geometry for reaction 6. Relevant distances (angstroms) and spin densities larger than 0.10 in absolute value (atomic units) are depicted. The leftmost carbon atom corresponds to C12 of the substrate

The first characteristic step in the combined radical/carbocation mechanism: 1,4 sigmatropic shift

In the radical/carbocation mechanism, O_2 addition to C11 is preceded by a series of events triggered by hydrogen transfer from C10 to the C13-based radical. The transition state of this reaction is shown in Fig. 7. The spin distribution in this structure is almost symmetrical, as are the C10–H and C13–H distances. As in the other reactions described, the transferred hydrogen atom carries almost no spin. Still, its spin of 0.08 is the largest of those found on transferred hydrogen atoms in this study. The activation free energy of this reaction, 36.5 kcal/mol, more than 20 kcal/mol higher than the experimental barrier, effectively discards this mechanism for the cyclooxygenase reaction.

Conclusions

Our results show that the proposed radical-only pathway but not the combined radical/carbocation mechanism for PGG_2 synthesis from arachidonic acid by PGHS is fully compatible with the experimentally observed kinetics (Fig. 8). Two steps (the initial hydrogen abstraction by Tyr385 and the closing of the peroxo bridge in the third step) were found to have activation free energies very close to the expected value of 15.0 kcal/mol. The calculations, however, do not allow us to decide which of these steps is rate-determining in the enzyme. The intervention of the amino acids excluded from our models is not required for the proposed reaction mechanism to be kinetically feasible. It thus appears that apart from the initial, very specific, 13-pro-S hydrogen abstraction, the role of the active site of the enzyme is mostly to force the substrate to adopt a conformation conducive to the synthesis of PGG_2, as suggested by experimental studies [5].

As this paper was being submitted, Blomberg et al. [24] reported a theoretical study of the radical-only mechanism of arachidonic acid cyclooxygenation. Although the overall shape of the potential-energy surface is similar in both reports, several differences were also found. In particular, the calculated activation free energies in Ref. [24] are consistently 2–3 kcal/mol lower than the ones we obtained. The transition state in step 1 is also different in both reports: in our model, the C13–H and O–H bonds have identical lengths (1.18–1.20 Å) and are shorter than the ones reported in Ref. [24] (1.25 and 1.37 Å, respectively). Both differences can probably be attributed to the different basis sets used in both studies [d95v in Ref. [24] versus our use of 6-31G(d)]. As in our calculations, the study of Blomberg et al. found that besides the initial hydrogen abstraction, a second step also has an activation energy close to the experimental value, although in their case this step was the formation of the C8–C12 bond, rather than the formation of the peroxo bridge. Additional models including the steric effects of additional amino acids in the active site will probably be needed to discriminate between both hypotheses.

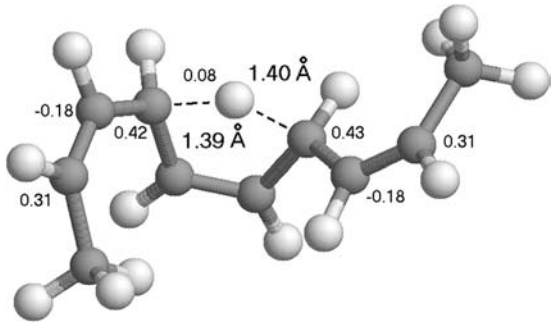

Fig. 7. Optimized transition-state geometry for the proposed 1,4-sigmatropic shift preceding substrate oxidation in the combined radical/carbocation mechanism. Relevant distances (angstroms) and spin densities larger than 0.10 in absolute value (atomic units) are depicted. The leftmost carbon atom corresponds to C16 of the substrate

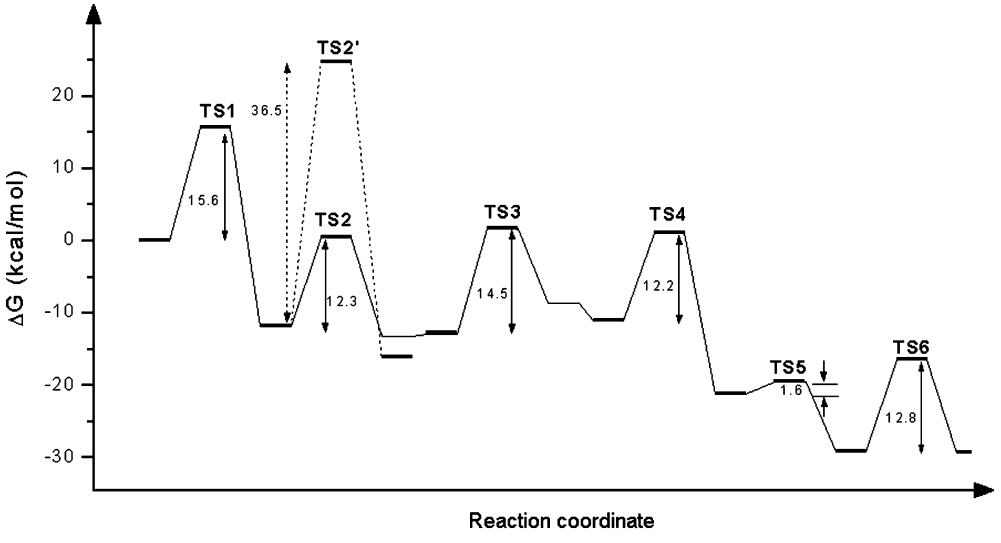

Fig. 8. The calculated free-energy surfaces for the radical-only (*solid line*) and combined radical/carbocation mechanisms (*dashed line*)

References

Marnett LJ, Rowlinson SW, Goodwin DC, Kalgutkar AS, Lanzo CA (1999) J Biol Chem 274:22903

Smith WL, DeWitt DL, Garavito RM (2000) Annu Rev Biochem 69:145

Kurumbail RG, Kiefer RJ, Marnett LJ (2001) Curr Opin Struct Biol 11:752

Malkowski MG, Ginell SL, Smith WL, Garavito RM (2000) Science 289:1933

Thuresson ED, Lakkides KM, Rieke CJ, Sun Y, Wingerd BA, Micielli R, Mulichak AM, Malkowski MG, Garavito RM, Smith WL (2001) J Biol Chem 276:10347

Hamberg M, Samuelsson B (1967) J Biol Chem 242:5336–5343

Goodwin DC, Gunther MR, Hsi LC, Crews BC, Eling TE, Mason RP, Marnett LJ (1998) J Biol Chem 2738903

Tsai A-L, Palmer G, Xiao G, Swinney DC, Kulmacz RJ (1998) J Biol Chem 273:3888

Dean AM, Dean FM (1999) Protein Sci 8:1087

Peng S, Okeley NM, Tsal A-L, Wu G, Kulmacz RJ, van der Donk WA (2002) J Am Chem Soc 124:10785

Becke AD (1993) J Chem Phys I 98:5648

Lee C, Yang W, Parr R (1998) J Phys Rev B 37:785

Hertwig RW, Koch W (1995) J Comput Chem 16:576

Siegbahn PEM, Eriksson L, Himo F, Pavlov M (1998) J Phys Chem B 102:10622

Fernandes PA, Ramos MJ (2003) J Am Chem Soc 125:6311

Fernandes PA, Eriksson L, Ramos MJ (2002) Theor Chem Acc 108:352

Forrester J, Frisch A (1996) Exploring chemistry with electronic structure methods. Gaussian, Pittsburgh, pp 64, 157

Barone V, Cossi M (1998) J Phys Chem A 102:1995–2001

Frisch MJ, Trucks GW, Schlegel HB, Scuseria GE, Robb MA, Cheeseman JR, Zakrzewski VG, Montgomery JA Jr, Stratmann RE, Burant JC, Dapprich S, Millam JM, Daniels AD, Kudin KN, Strain MC, Farkas O, Tomasi J, Barone V, Cossi M, Cammi R, Mennucci B, Pomelli C, Adamo C, Clifford S, Ochterski J, Petersson GA, Ayala PY, Cui Q, Morokuma K, Malick DK, Rabuck AD, Raghavachari K, Foresman JB, Cioslowski J, Ortiz JV, Baboul AG, Stefanov BB, Liu G, Liashenko A, Piskorz P, Komaromi I, Gomperts R, Martin RL, Fox DJ, Keith T, Al-Laham MA, Peng CY, Nanayakkara A, Challacombe M, Gill PMW, Johnson B, Chen W, Wong MW, Andres JL, Gonzalez C, Head-Gordon M, Replogle ES, Pople JA (1998) Gaussian 98, revision A.9. Gaussian, Pittsburgh, PA

Blomberg MRA, Siegbahn PEM, Babcock GT (1998) J Am Chem Soc 120:8812

Mulliken RS (1955) J Chem Phys 23:1833

Lehnert N, Solomon EI (2003) J Biol Inorg Chem 8:294

Kulmacz RJ, Pendelton RB, Lands WEM (1994) J Biol Chem 269:5527

Blomberg LM, Blomberg MRA, Siegbahn PEM, van der Donk WA, Tsai A-L (2003) J Phys Chem B 107:3297